(Preprint) AAS 24-385

DESIGN OF SAFETY PROCEDURE FOR A MULTI-SATELLITE FORMATION USING A CONTINUOUS CONTROL SCHEME

Francesca Scala,[*] Gerhard Krieger,[†] and Michelangelo Villano[‡]

The concept of multiple satellites in formation represents a significant advancement in enhancing the capabilities of synthetic aperture radar interferometry. Maintaining the correct baseline and a safe configuration among the vehicles is vital for high-resolution across-track SAR interferometry missions. This study focuses on across-track single-pass interferometry, based on fixed time-invariant baselines, and introduces a novel guidance and control strategy specifically designed to address safety procedures in case of off-nominal onboard conditions. The research examines the capability for rapid formation reconfiguration to enter safe mode in terms of minimum propellant consumption and passive safety.

INTRODUCTION

In the past decade, the capability to produce accurate digital elevation models (DEMs) for precise measurements of Earth's geophysical parameters has improved thanks to distributed missions in low Earth orbits (LEO). The TanDEM-X mission exemplified the effectiveness of distributed systems, particularly in the context of single-pass across-track interferometry.[1] Starting from these findings, this paper focuses on distributed systems of three or more satellites for across-track interferometry, based on fixed baselines, opening many applications to enhance future SAR missions.[2] Maintaining a constant or quasi-constant separation between the satellites is paramount for achieving high-resolution acquisitions for SAR interferometry. We implemented a continuous control scheme to keep the formation configuration and follow the guidance trajectory, while ensuring a safe configuration throughout the duration of the mission. [2] The proposed approach is based on model predictive control (MPC), a powerful technique capable of predicting future system behavior and optimizing control actions accordingly. In recent years, multiple solutions based on MPC have been provided in literature studies, demonstrating the advantages and disadvantages of the methodology.[3] Specifically, MPC offers advantages such as robustness to disturbances and the ability to handle constraints in the algorithm's formulation. Additionally, thanks to the mathematical representation in convex formulation, it ensures sub-optimal solutions in terms of control profile. The fuel optimal MPC formulation was proposed in the literature, to address on-board implementation with collision avoidance constraints.[4] Later, multiple optimal guidance solutions with MPC were studied for a swarm of satellites in combination with earth's oblateness J_2 invariant orbits and collision avoidance constraints.[5,6] These studies open the investigation for different applications

[*] Post-Doctoral Researcher, Microwaves and Radar Institute, German Aerospace Center (DLR), Münchener Straße 20, 82234 Weßling, Germany.
[†] Head of Department Radar Concepts, Microwaves and Radar Institute, German Aerospace Center (DLR), Münchener Straße 20, 82234 Weßling, Germany.
[‡] Leader of the NewSpace SAR Group, Microwaves and Radar Institute, German Aerospace Center (DLR), Münchener Straße 20, 82234 Weßling, Germany.

involving formation flying, specifically addressing the need for autonomous task assignment strategies and autonomous reconfiguration procedure in orbit.[7,8] Both these studies were based on the representation of the relative dynamics in the chief-centered Hill relative frame and were devoted to the computation of optimal guidance trajectories without the implementation of the MPC. More recent studies further couple the representation of the dynamics in the Relative Orbital Elements (ROE) together with optimal guidance solutions with MPC. A maneuver planning algorithm for satellite formations using mean relative orbital elements was proposed for a distributed system of satellites to assess the fuel consumption performances.[9] Then, relative and absolute orbit control in a high-drag environment was investigated in the ROE framework based on MPC algorithms.[10] These recent works are based on the dynamical representation in the ROE framework, to better include the external perturbation in the state transition matrix. Additionally, they all include collision avoidance constraints among the satellites in the distributed system, to ensure safety during orbit operations. Following the previous works in the literature, we developed a dynamical model for the MPC, incorporating the main external perturbations in the LEO region, to accurately represent the orbital environment, such as the Earth's oblateness (J_2) and the atmospheric drag, including seasonal variations. The dynamical model is based on ROE representation to better handle external perturbations and safety considerations. Additionally, unlike previous studies, we specifically tailor the control technique for formation reconfiguration scenarios when short satellite distances are involved (< 100 m). For such scenarios, the safety procedure during orbital operations becomes of paramount importance, and the ROE representation allows a formulation of the safety conditions even in case of malfunctioning or loss of control.[11] For this purpose two scenarios were simulated, considering the full thrust capability of the formation, and subsequently, the case of engine failure to address the need of reconfiguration in the safe mode with reduced control capabilities.

METHODOLOGY

The work focuses on guidance and control (G&C) strategies employing low-thrust engines within an MPC control scheme. Various scenarios are analyzed for the transition between the scientific SAR interferometry configuration and the safe configuration in response to undesired behavior or detection of collision risk. The proposed G&C approach adopts a decentralized architecture for the autonomous management of the formation by each vehicle of the distributed system, removing the need for control from a reference spacecraft. Throughout the simulation, we assume an onboard navigation system based on GNSS differential measurements for precise estimation of the current state of the formation.[12] Additionally, the platforms have the same processing capabilities to handle the required computation from onboard sensors and actuators.

Dynamics Model

The relative motion of multiple satellites flying in formation is described in terms of quasi-nonsingular ROE, as introduced in D'Amico (2010).[13] To describe the relative motion, the absolute orbit of the main satellite is identified by non-singular Keplerian elements $\boldsymbol{el}_c = \{a, \lambda, e_x, e_y, i, \Omega\}_c$. Similarly, the non-singular Keplerian elements of the j-th secondary satellite are $\boldsymbol{el}_j = \{a, \lambda, e_x, e_y, i, \Omega\}_j$. The quantity $\lambda = \omega + M$ is the mean argument of latitude depending on the argument of perigee ω and mean anomaly M, and $\{e_x, e_y\}$ are the x and y components of the eccentricity vector, $e\cos\omega$ and $e\sin\omega$, respectively. From this representation, the ROEs are:

$$\boldsymbol{\delta\alpha}_j = \begin{Bmatrix} \delta a \\ \delta\lambda \\ \delta e_x \\ \delta e_y \\ \delta i_x \\ \delta i_y \end{Bmatrix}_j = \begin{Bmatrix} (a_j - a_c)/a_c \\ \lambda_j - \lambda_c + (\Omega_j - \Omega_c)\cos i_c \\ e_{x_j} - e_{x_c} \\ e_{y_j} - e_{y_c} \\ i_j - i_c \\ (\Omega_j - \Omega_c)\sin i_c \end{Bmatrix}, \tag{1}$$

where δa_j is the relative semi-major axis, $\delta\lambda_j$ is the relative mean argument of latitude, δe_{x_j} and δe_{y_j} are the x and y components of the relative eccentricity vector $\boldsymbol{\delta e_j}$, whereas δi_{x_j} and δi_{y_j} are the x and y components of the relative inclination vector $\boldsymbol{\delta i_j}$. To include the drag effect in the dynamics, we introduced an augmented state vector, including the drift $\delta\ddot{a}$ in the relative semi-major axis:

$$\boldsymbol{\delta a}^* = \{\delta a, \delta\lambda, \delta e_x, \delta e_y, \delta i_x, \delta i_y, \delta\ddot{a}\}. \tag{2}$$

From this representation, the linearized dynamics, including the control term for the j-th satellite of the formation is expressed as:

$$\boldsymbol{\delta\dot{\alpha}}^*(t) = \mathbf{A}(t, t_0)\boldsymbol{\delta\alpha}^*(t_0) + \boldsymbol{B}(t)\boldsymbol{u}(t), \tag{3}$$

where the matrix $\mathbf{A}(t, t_0)$ includes the differential effects of the Keplerian motion, the Earth's oblateness and the atmospheric drag; while the matrix $\boldsymbol{B}(t)$ is the control matrix, and the vector $\boldsymbol{u}(t)$ is the control input in the relative Hill frame.

Keplerian Motion. The unperturbed contribution from Keplerian motion is based on the Hill-Clohessy-Wiltshire equations and can be expressed as:

$$\boldsymbol{A_{hcw}}(t) = \begin{bmatrix} 0 & \\ -1.5\,n & \mathbf{0_{2\times5}} \\ \mathbf{0_{4\times1}} & \mathbf{0_{4\times5}} \end{bmatrix}, \tag{4}$$

where the quantity $\mathbf{0}_{n\times m}$ is the matrix full of zeros with dimensions $\{n, m\}$, t is the time variable, and n is the mean motion of the primary orbit.

Differential Earth Oblateness and Atmospheric Drag Effects. The component including the effects of J_2 and differential drag is defined as:

$$\boldsymbol{A_{j2,dd}}(t) = \begin{bmatrix} \mathbf{A_{j2}}(t) & \mathbf{A_{dd}}(t) \\ \mathbf{0_{1\times6}} & 1 \end{bmatrix}, \tag{5}$$

where $\mathbf{A}_{j2}$ is the part including the Earth's oblateness effect, and $\mathbf{A}_{dd}$ is connected to the differential drag. The full expression of the matrix $\boldsymbol{A_{j2,dd}}(t)$ can be found in Koenig et al. (2017).[14] In this work we consider the Schatten model for the solar cycle prediction.[15] We also adopted the NRLMSISE empirical model of the atmosphere, that incorporates the information on A_p and $F_{10.7}$, for the definition of the atmospheric density as function of the altitude.[16]

Control Accelerations. The control matrix $\boldsymbol{B}(t)$ was derived to map the control accelerations $\boldsymbol{u}(t)$ from the Hill reference frame to the ROE framework. Its expression and its full derivation can be found in Steindorf et al (2017).**Error! Bookmark not defined.**

Model Predictive Control

Similar to previous works,[9,10,11] the proposed approach employs MPC as a feedback control, formulating the control objective as linear and quadratic expressions to identify the most fuel-efficient spacecraft maneuver. The control actions fed to the control system consist of a specific subset of the optimal control problem's global solution. The relative dynamic is modeled in terms of relative orbital elements (ROEs) to better include the constraints in terms of collision avoidance.[11]

MPC Control Logic. The MPC is implemented as a feedback algorithm that accounts for mismatch and inaccuracies between the current states and the optimal guidance, due to external disturbances not included in the analytical model of the relative dynamics. Specifically, at each step, the optimal guidance trajectory is computed as the solution of an open-loop optimal control and the commanded control is implemented in the following step. The control logic is illustrated in Figure 1. Following the procedure in Morgan et al. (2014), the dynamical system in Eq. 3 can be discretized and divided into finite time steps dt, with a piece-wise constant control in each time step.[5] At the initial time step of the maneuver, the algorithm computes the initial optimal guidance in terms of optimal trajectory and control profile. The solution at the initial step serves as the initial

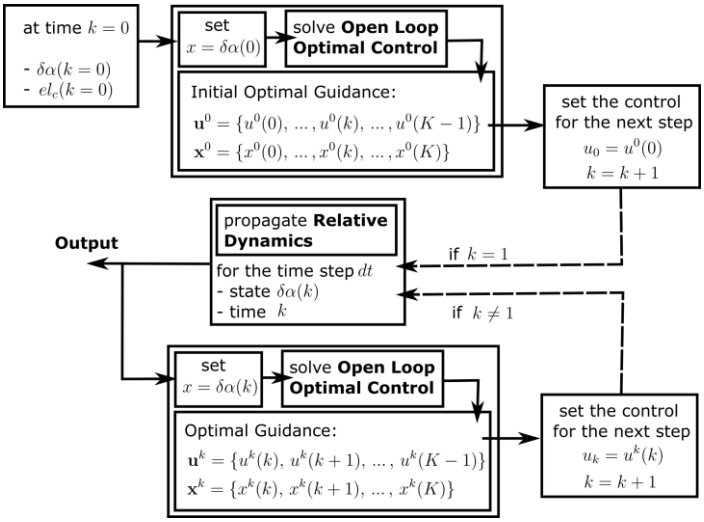

Figure 1. Flow diagram for the model predictive control.

conditions for the state update and to start the repetitive use of the open loop optimal control at each subsequent time step. The MPC computes the optimal guidance at each time instance k (with $k = 1, \dots, K$) and state $\delta\alpha(k)$; then, the control at the considered state is set equal to the first term of a related optimal sequence of control actions u^k. This way of proceeding improves the stability of the optimal maneuver and the inclusion in the relative dynamic model of uncertainties and additional external perturbations (e.g. navigation uncertainties, high-fidelity orbital perturbations).[3]

Open Loop Optimal Control. The solution of the open loop optimal control is based on the linearization and discretization of the cost function, the system dynamics, and system constraints. In particular, we follow the derivation of the control problem based on the convexification of each term.[7,8,9] The decisional vector of the optimization is defined including the state and the control vectors for each satellite in the formation. Assuming a distributed system with $j = 1, \dots, N$ number of deputies, the decisional vector is defined as:

$$\widehat{\boldsymbol{X}} = \left\{\delta\boldsymbol{\alpha}_1, \boldsymbol{u}_1, \dots, \delta\boldsymbol{\alpha}_j, \boldsymbol{u}_j, \dots, \delta\boldsymbol{\alpha}_N, \boldsymbol{u}_N\right\}, \tag{6}$$

where $\delta\boldsymbol{\alpha}_j, \boldsymbol{u}_j$ contain the state and the control vector for each time step k, with dimensions $7K$ and $3(K-1)$, respectively. The cost function to be minimized can be expressed in terms of the decisional state vector and aims at minimizing the control effort for the optimal maneuver. We have considered the following cost function:[8]

$$J = \sum_1^K \left\|\boldsymbol{u}_j[k]\right\|, \tag{7}$$

where this expression corresponds to the minimization of the fuel consumption during the maneuver. After the definition of the cost function, it is important to properly identify and define the constraints of the control system. First, the relative dynamic under forced motion is included in the system, as:

$$\delta\boldsymbol{\alpha}_j[k+1] = (\boldsymbol{I} + \boldsymbol{A}[k]\, dt)\delta\boldsymbol{\alpha}_j[k] + \boldsymbol{B}[k]\, dt\, \boldsymbol{u}_j[k], \tag{8}$$

Similarly, we impose the initial and final condition on the relative state of the formation as:

$$\delta\boldsymbol{\alpha}_j[k=1] = \delta\boldsymbol{\alpha}_{j,0} \qquad \delta\boldsymbol{\alpha}_j[k=K] = \delta\boldsymbol{\alpha}_{j,f}. \tag{9}$$

Finally, we have considered the limitation on the control acceleration that the thruster can provide and the constraint on the collision avoidance among the satellites in the formation. The former is connected to the technological limitation of the on-board engine, and it is expressed as:

$$\left\|\boldsymbol{u}_j[k]\right\| \leq \boldsymbol{u}_{\mathbf{max_j}}. \tag{10}$$

The latter, instead, is of paramount importance to ensure a safe reconfiguration. Its formulation was derived following the procedure identified in previous works. Its convex formulation is:

$$\left(\boldsymbol{L}[k]\delta\bar{\boldsymbol{\alpha}}_{\boldsymbol{j}}[k]-\boldsymbol{L}[k]\delta\bar{\boldsymbol{\alpha}}_{\boldsymbol{i}}[k]\right)^{T}\left(\boldsymbol{L}[k]\delta\boldsymbol{\alpha}_{\boldsymbol{j}}[k]-\boldsymbol{L}[k]\delta\boldsymbol{\alpha}_{\boldsymbol{i}}[k]\right)\geq d_{coll}\left\|\boldsymbol{L}[k]\delta\bar{\boldsymbol{\alpha}}_{\boldsymbol{j}}[k]-\boldsymbol{L}[k]\delta\bar{\boldsymbol{\alpha}}_{\boldsymbol{i}}[k]\right\|, \quad (11)$$

where $\delta\bar{\boldsymbol{\alpha}}_{\boldsymbol{j}}$ and $\delta\bar{\boldsymbol{\alpha}}_{\boldsymbol{i}}$ refer to the optimal solution found at the previous MPC iteration. Note that the constraint on the inter-satellite collision avoidance is based on the knowledge of the predicted trajectory evolution. For this reason, the solution of the open loop optimal control at the very first step is different from the subsequent steps, as the predicted trajectory is not yet available. Therefore, only for the first step, the optimal solution is first computed without including the collision avoidance constraint. Then, this solution is used as input for a second iteration to obtain an optimal trajectory compliant with the collision avoidance constraint. The matrix $\boldsymbol{L}[\boldsymbol{k}]$ is introduced to retrieve the inter-satellite relative distance from the ROE state of satellite i and satellite j at each time instant k. The solution of the open loop optimal control is computed following the formulation of the CVXPY Python-embedded modeling language for convex optimization problems, which is defined and solved with open-source available algorithms (e.g. CLARABEL or MOSEK).

SIMULATIONS

The case under analysis consists of a formation of three spacecraft in a fixed baseline configuration. During the SAR acquisition phase, a continuous thrust is essential to keep the spacecraft separation, particularly with small fixed baselines (< 100 m), which is promising in combination with antennas operating in the Ka-band of the electromagnetic spectrum, due to their low penetration in the terrain.[2,17]

Simulation Scenarios

The proposed analysis provides a baseline procedure for assessing the G&C performances of multiple satellites flying in close proximity. It provides assessments of the control accuracy and the total delta-velocity cost, considering two case scenarios. In *Scenario 1*, we assume that the low-thrust engines correctly function for the whole formation. The MPC is designed to assess a reconfiguration from the SAR acquisition configuration to the safe mode in a predefined time frame, keeping the thrust level below the maximum capability of the engine and a minimum distance among the spacecraft. The performances of this scenario are compared with *Scenario 2*, where engine failure is simulated. In this case, the simulation aims to demonstrate the feasibility of maneuvering to the safe mode even when one spacecraft loses its control capability. The parameters and boundary conditions for the simulation scenarios are reported in Table 1. The initial conditions correspond to the formation geometry under a fixed baseline configuration.[2] We have considered two deputies with a baseline purely in the across-track direction of the Hill reference frame, with no separation in radial or along-track directions. This configuration can be kept under the assumption of continuous forced motion.[2] This is a non-passive safe configuration that could result in an unsafe condition in case of non-nominal or failure situations. The relative eccentricity and inclination vectors are not (anti-) parallel, and the safety of the formation must be achieved through onboard autonomous formation reconfiguration.[18] The final condition after the maneuver is selected to respect the (anti-) parallel condition of relative eccentricity and inclination vectors for passive safety, resulting in the well know Helix relative trajectory.[18] The maneuver time was selected below one orbital period to ensure a fast reconfiguration to the safe mode.

Formation Reconfiguration with Full Engine Capability

The first scenario aims at designing an optimal maneuver to reconfigure the formation from the initial to final condition using the MPC procedure described in Figure 1. To evaluate the robustness of the solution, we have run the MPC considering an error in the initial condition $a\delta\boldsymbol{\alpha}_{\boldsymbol{j.0}}$ to simulate

navigation and control uncertainties. We simulated the reconfiguration of 10 initial conditions with a maximum error of ± 50 cm for the relative semi-major axis and mean argument of latitude, and a maximum error of $\pm$ 10 cm for the components of the relative eccentricity and inclination vector. The error in the evolution of the relative eccentricity and inclination vectors during the reconfiguration maneuver is shown in Figure 2 (left), where the results of 10 simulations have been reported. The initial difference in the y components of δe and δi converges to zero during the reconfiguration. Figure 2 (right) shows the relative trajectory in time for one of the 10 initial conditions, where the initial and final formation geometry is propagated for 2 orbit periods, and the maneuver phase is shown with a bold segment. The trajectory of the chief at the center of the formation is represented by a dotted grey line. We can observe how in the initial leg, the across-track position is kept constant to guarantee a fixed baseline for SAR interferometry.[2] The optimal maneuver reconfigures the deputies into two nested helix relative trajectories, which are propagated for two orbital periods after the maneuver. Looking then at the time evolution of the x and y components of the relative eccentricity and inclination vector, the maneuver imposes a change to set a parallel $\delta e/\delta i$ for both deputies, as shown in Figure 3 (left). Multiple works demonstrated that this condition ensure a passively safe relative motion.[11,13,18] Finally, the commanded thrust profile during the maneuver is shown in Figure 3 (right). Considering the condition in Table 1 and a spacecraft mass of 500 kg, the maximum thrust level for the maneuver is set equal to 15 mN, represented by the dotted yellow line in the graphic. The reconfiguration is possible considering such limitation for both deputies 1 and 2, under the assumption of full engine capabilities on-board. In a next analysis, the feasibility of the thrust profile in the body frame will be investigated.

Table 1. Scenarios parameters and boundary conditions

Initial Conditions	$a\delta\boldsymbol{\alpha}_{j.0}$	$j=1\ \{0,0,0,0,4,-40\}$ $j=2\ \{0,0,0,0,-4,20\}$	Maneuver time	T_f	0.8 Period
Final Conditions	$a\delta\boldsymbol{\alpha}_{j.f}$	$j=1\ \{0,0,0.5,-60,0.5,-60\}$ $j=2\ \{0,0,-0.5,30,-0.5,30\}$	Number of time steps	K	100
Chief's orbit	$\boldsymbol{el_c}$	{775 km, 8e-5, 5e-5, 98.5 deg, 30 deg, 0 deg}	Max thruster acceleration	$\boldsymbol{u_{max_j}}$	3e-5 m/s^2
			Safety distance	d_{coll}	7.5 m

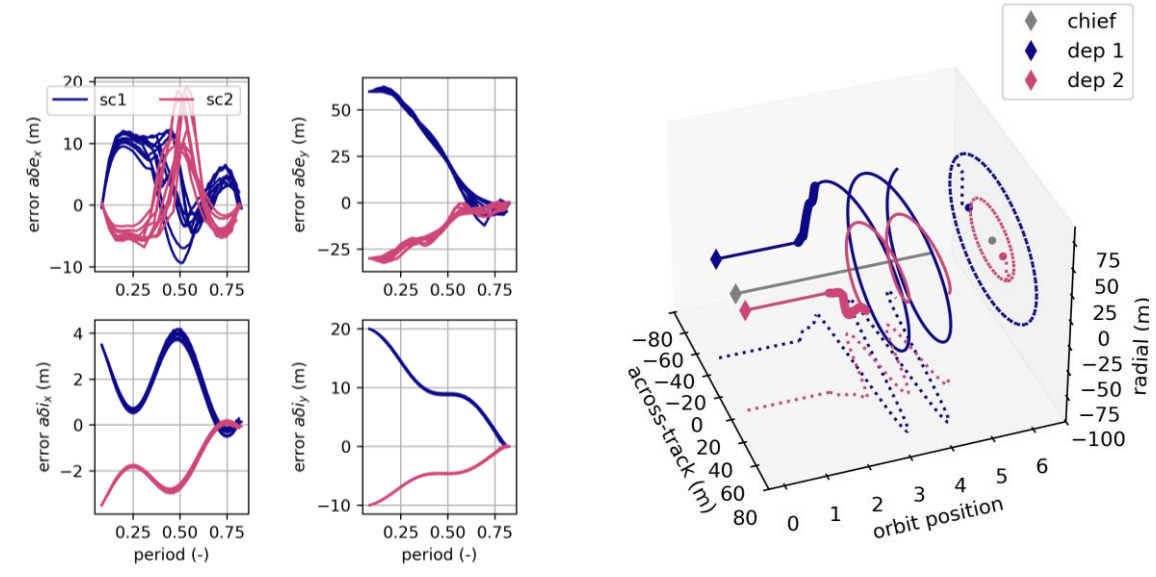

Figure 2. Error during the reconfiguration maneuver for 10 initial conditions (left). Time evolution of the reconfiguration maneuver from fixed baseline to helix geometry (right).

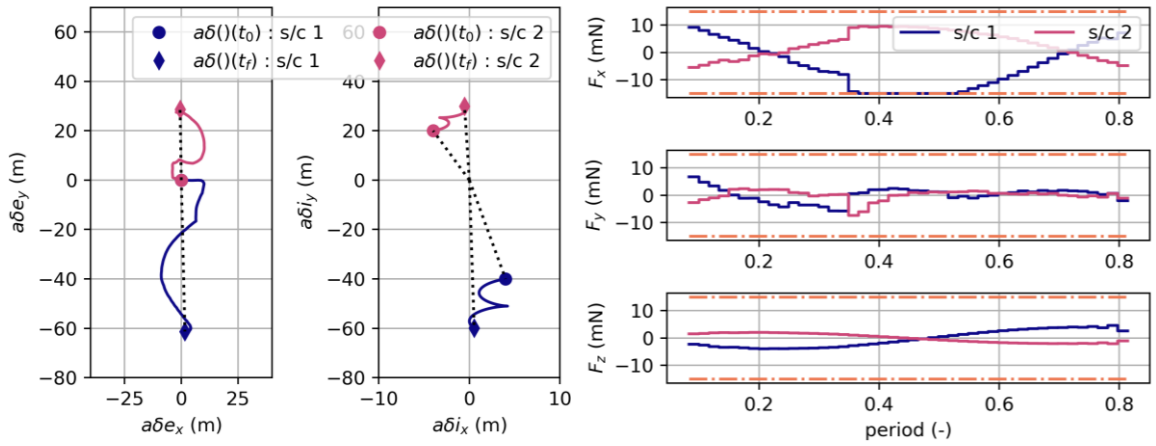

Figure 3. Evolution of the $a\delta e$ and $a\delta i$ during the maneuver (left). Command thrust profile during the maneuver (right).

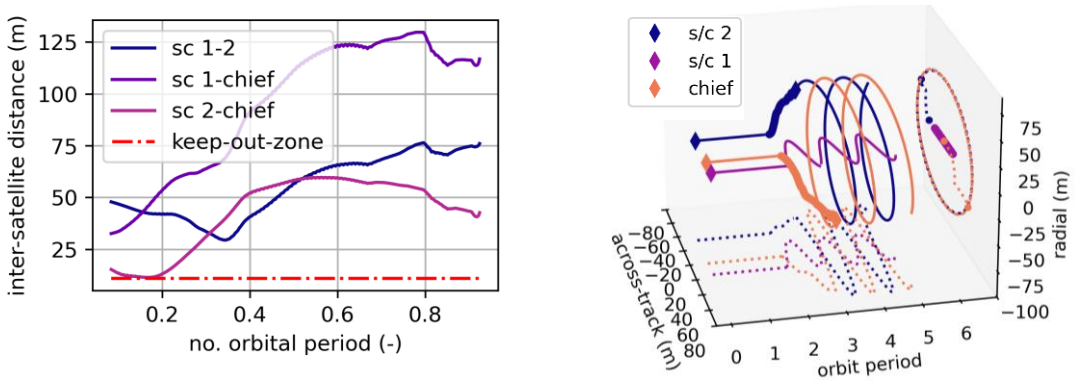

Figure 4. Inter-satellite distance during the reconfiguration maneuver (left) and time evolution of the reconfiguration maneuver (right) under loss of control of the spacecraft 1.

Safe Formation Acquisition under Engine Failure

The second scenario under analysis considers the same initial conditions and parameters of Table 1. We assume the engine failure for deputy no. 1, and that it cannot control its relative trajectory. Due to the nature of the fixed baseline configuration defined by the initial conditions, once one of the deputies loses the controllability, its relative motion undergoes a natural oscillation in the across-track trajectory. This behavior generates a collision risk with the other satellites. As the deputy 1 is subject to a failure of one of the engines and cannot control its trajectory, an alert message should be transmitted from deputy 1 to the other satellites via an omni-directional radio-frequency transmission. Then, the deputy 2 and the chief satellite immediately implement a maneuver to move away and reconfigure to a helix geometry. During the safety maneuver, the deputy 2 and the chief account for the natural motion of the deputy 1 and optimize the maneuver accordingly. The evolution in time of the distance during the maneuver among each platform of the distributed system is shown in Figure 4 (left). We can observe how the minimum distance is respected in the simulation. Similarly, Figure 4 (right) shows the time evolution of the across-track and radial components of the trajectory during the 3 phases: 1. fixed baseline for two orbital periods, 2. loss of controllability by spacecraft 1 and maneuver of spacecraft 2 and chief satellite, 3. Insertion of spacecraft 2 and chief satellites in the helix formation and uncontrolled motion of satellite 1.

CONCLUSIONS

In this paper, the proposed approach investigates the safety of flying two or more platforms in close proximity for potential across-track SAR interferometry applications. Having a short baseline among the satellites can be beneficial for various applications, especially when using the Ka-band frequency. As shown in previous works, the concept of keeping a short-fixed baseline poses some risks and uncertainties on the safety of the formation. This aspect prompts an investigation into the feasibility of the reconfiguration into a passive safe geometry, such as the helix relative orbit, using an MPC control scheme. The simulations have shown that the reconfiguration maneuver to the safe mode can be achieved promptly, in less than one orbital period, with a low thrust control scheme. This was simulated with the full control capability of the satellites, and even in the event of propulsion system failure in one of the deputies. In the latter case, where one satellite loses controllability, the other spacecraft in the formation executes an evasive maneuver to reach a safe position and avoid potential collision risk. Furthermore, the MPC algorithm was developed based on a linearized model of the dynamics to reduce the computational effort during the optimal open loop control, in view of implementing the approach directly in the on-board routine to move towards autonomous GNC.

ACKNOWLEDGMENTS

This work was partially funded by the European Union (ERC Starting Grant Distributed Radar Interferometry and Tomography Using Clusters of Smallsats (DRITUCS) 101076275). Views and opinions expressed are however those of the authors only and do not necessarily reflect those of the European Union or the European Research Council Executive Agency. Neither the European Union nor the granting authority can be held responsible for them.

REFERENCES

[1] G. Krieger, A. Moreira, H. Fiedler, I. Hajnsek, M. Werner, M. Younis, and M. Zink, "TanDEM-X: A satellite formation for high-resolution SAR interferometry," *IEEE Transactions on Geoscience and Remote Sensing*, vol. 45, no. 11, pp. 3317-3341, Nov. 2007, doi: 10.1109/TGRS.2007.900693

[2] F. Scala, G. Krieger, and M. Villano, "Investigation of Fixed Across-Track Baselines for Distributed Spaceborne SAR Systems." *15th European Conference on Synthetic Aperture Radar (EUSAR 2024)*, Munich (Germany), April 23-26, 2024.

[3] U. Eren, A. Prach, B. B. Koçer, S. V. Raković, E. Kayacan, and B. Açıkmeşe, "Model predictive control in aerospace systems: Current state and opportunities." *Journal of Guidance, Control, and Dynamics*, vol. 40, no 7, pp. 1541-1566, July 2017, doi: 10.2514/1.G002507.

[4] B. Acikmese, D. Scharf, F. Hadaegh, and E. Murray. "A convex guidance algorithm for formation reconfiguration." In *AIAA Guidance, Navigation, and Control Conference and Exhibit*, 21-24 August 2006, Keystone, Colorado (USA), pp. 6070, doi: 10.2514/6.2006-6070

[5] D. Morgan, S. J. Chung, and F. Y. Hadaegh, "Model predictive control of swarms of spacecraft using sequential convex programming." *Journal of Guidance, Control, and Dynamics*, vol. 37, no. 6, pp. 1725-1740, Oct. 2014, doi: 10.2514/1.G000218.

[6] A. Weiss, M. Baldwin, R. S. Erwin, and I. Kolmanovsky, I. "Model predictive control for spacecraft rendezvous and docking: Strategies for handling constraints and case studies." *IEEE Transactions on Control Systems Technology*, vol. 23, no. 4, pp. 1638-1647, July 2015, doi: 10.1109/TCST.2014.2379639.

[7] S. Sarno, J. Guo, M. D'Errico, and E. Gill, "A guidance approach to satellite formation reconfiguration based on convex optimization and genetic algorithms." *Advances in Space Research*, vol. 65, no. 8, pp. 2003-2017, Apr. 2020, doi: 10.1016/j.asr.2020.01.033.

[8] F. Scala, G. Gaias, C. Colombo, M. Martín-Neira, “Design of optimal low-thrust manoeuvres for remote sensing multi-satellite formation flying in low Earth orbit.” *Advances in Space Research*, vol. 68, no. 11, pp. 4359-4378, Dec. 2021, doi: 10.1016/j.asr.2021.09.030.

[9] A. M. Miñan, F. Scala, and C. Colombo, C., “Manoeuvre planning algorithm for satellite formations using mean relative orbital elements.” *Advances in Space Research*, vol. 71, no. 1, pp. 585-603, Jan 2023, doi: 10.1016/j.asr.2022.09.043.

[10] E. Belloni, S. Silvestrini, J. Prinetto, M. Lavagna, “Relative and absolute on-board optimal formation acquisition and keeping for scientific activities in high-drag low-orbit environment”, *Advances in Space Research*, vol. 71, no 11, pp. 5595-5613, June 2024, doi: 10.1016/j.asr.2023.07.051.

[11] G. Borelli, G. Gaias, and C. Colombo, “Safety in forced motion guidance for proximity operations based on relative orbital elements.” In *33rd AAS/AIAA Space Flight Mechanics Meeting*, January 15-19, Austin, Texas, pp. 1-19, no. AAS 23-142, 2023.

[12] V. Capuano, A. Harvard, and S. Chung, “On-board cooperative spacecraft relative navigation fusing GNSS with vision.” *Progress in Aerospace Sciences*, vol 128, pp. 100761, Jan 2022, doi: 10.1016/j.paerosci.2021.100761.

[13] S. D'Amico, “Autonomous formation flying in low earth orbit.” *Doctoral dissertation*, TU Delft, Delft, The Netherlands, 2010.

[14] A. W. Koenig, T. Giuffanti, and S. D’Amico. "New State Transition Matrices for Spacecraft Relative Motion in Perturbed Orbits," *Journal of Guidance, Control, and Dynamics*, vol. 40, no. 7, pp. 1749-1768, 2017, doi:10.2514/1.G002409.

[15] W.D. Pesnell, and K. H. Schatten, “An Early Prediction of the Amplitude of Solar Cycle 25,” *Sol. Phys*., vol 293, no. 112, 2018, doi: 10.1007/s11207-018-1330-5.

[16] J. M. Picone, A. E. Hedin, D. P. Drob, and A. C. Aikin, “NRLMSISE-00 empirical model of the atmosphere: Statistical comparisons and scientific issues,” Journal of Geophysical Research: Space Physics, vol 107, no. A12 pp. SIA 15-1-SIA 15-16, doi: 10.1029/2002JA009430.

[17] A. Moreira, P. Prats-Iraola, M. Younis, G. Krieger, I. Hajnsek and K. P. Papathanassiou, "A tutorial on synthetic aperture radar," *IEEE Geoscience and Remote Sensing Magazine*, vol. 1, no. 1, pp. 6-43, March 2013, doi: 10.1109/MGRS.2013.2248301.

[18] S. D'Amico, and O. Montenbruck, “Proximity operations of formation-flying spacecraft using an eccentricity/inclination vector separation,” Journal of Guidance, Control, and Dynamics, vol. 29, no. 3, pp. 554-563, May 2012, doi: 10.2514/1.15114.